First publ. in: Journal of Low Temperature Physics 22 (1976), 1-2, pp. 61-84

Investigation of the Lifetime of Longitudinal Phonons at GHz Frequencies in Liquid and Solid ^{4}He

P. Berberich, P. Leiderer, and S. Hunklinger*

Physik-Department, Technische Universität München, Garching, Germany

(Received May 29, 1975)

The attenuation of longitudinal 1-GHz phonons was measured as a function of temperature in liquid ^{4}He at svp and at 23 bar as well as in hcp ^{4}He at 36 bar. The lifetime of the phonons which were generated by stimulated Brillouin scattering was determined optically by a probing light pulse. The results in liquid ^{4}He are discussed in terms of relaxation processes in the phonon and roton gas and are in good agreement with existing work. The attenuation in hcp ^{4}He, which approximately shows a T^4 temperature dependence, is attributed to three-phonon processes with longitudinal thermal phonons. A quantitative comparison with Landau–Rumer theory gives satisfactory agreement with the data. No effect of phonon dispersion on sound attenuation is found down to 0.8 K.

1. INTRODUCTION

Interactions between phonons in dielectric crystals are caused by the anharmonicity of the crystal lattice. This is well understood from traditional lattice dynamics first proposed by Born and von Karmann.[1] Here, the displacements of the atoms are regarded to be small compared to the interatomic spacings so that the potential energy may be expanded in powers of the displacements. Then the cubic terms of this expansion, which can be expressed by third-order elastic constants, introduce phonon–phonon interactions. One class of solids, the quantum crystals, cannot be treated in this way because the vibrational motion of the atoms is not small relative to the lattice spacing. This is most pronounced in solid helium. Therefore various experiments, such as sound velocity measurements[2–4] and neutron scattering experiments,[5,6] have been carried out in recent years to study

*Present address: Max Planck Institut für Festkörperforschung, B.P. 166 Centre de Tri, F-38 Grenoble, France.

the phonon dispersion curves of solid ^{4}He. Simultaneously the theoretical treatment of quantum crystals has been improved (see, e.g., Ref. 7). Using self-consistent phonon theory, Gillis *et al.*,[8] for example, calculated a phonon dispersion curve for hcp ^{4}He which was in satisfactory agreement with neutron scattering and sound velocity data.

Self-consistent phonon theory was also used by several authors[9–11] to calculate the phonon damping rate. However, only phonon decay processes were considered and no prediction for the ultrasonic attenuation at finite temperatures was made, where the interaction with thermal phonons is the main contribution. For finite temperatures Jäckle and Kehr[12] have found a solution in a completely different way. These authors do not determine the phonon damping rate from the bare interatomic potential and its anharmonicity, but they show that the damping of the phonons in a quantum crystal can be expressed in terms of *effective* anharmonic interactions which are given by the higher order elastic constants as in normal dielectric crystals. They predict that the ultrasonic attenuation at high frequencies is mainly determined by the three-phonon process (3PP). If Ω is the angular frequency of the sound wave and τ_{th} the thermal phonon lifetime, then near $T = 0$ ($\Omega \gg k_B T/\hbar$) the decay of the ultrasonic phonons is the dominant 3PP, while at higher temperatures ($1/\tau_{th} \ll \Omega \ll k_B T/\hbar$) the sound wave is mainly attenuated by a 3PP where an ultrasonic phonon combines with a thermal phonon to produce a thermal phonon of higher frequency.

It has been well established that this process, which was first considered by Landau and Rumer,[13] mainly contributes to the ultrasonic attenuation in many dielectric crystals at low temperatures.[14] After it was found that this mechanism is also responsible for sound absorption in liquid ^{4}He below 0.6 K (for a review see, e.g., Ref. 15), where longitudinal phonons are the only excitations present, this isotropic and almost defect-free substance has proved to be ideal for studying phonon–phonon interactions. Since energy and momentum must be conserved in the 3PP, the ultrasonic attenuation can be sensitive to phonon dispersion. In this field surprising results were obtained in liquid ^{4}He. So Maris and Massey[40] concluded from the ultrasonic experiments of Abraham *et al.*[37] in ^{4}He at svp that the phonon dispersion curve is anomalously bent upward. Jäckle and Kehr[23] could explain the uncommon results of Roach *et al.*[42] in liquid ^{4}He under pressure by assuming that the dispersion curve is initially bent upward but turns down to normal dispersion above a certain cutoff wave vector which shifts to smaller values with increasing pressure. An explanation for this behavior, which has been confirmed meanwhile by more direct methods,[56,57] has not been given until now. In this context it would be interesting to have some information about phonon dispersion in solid ^{4}He.

We want to report in this paper on a measurement of the ultrasonic attenuation at GHz frequencies in the quantum solid ^{4}He. Longitudinal

phonons were produced optically by stimulated Brillouin scattering and their lifetime was determined by a probing light pulse. We preferred this technique because conventional ultrasonics is known to be subject to large parasitic attenuation effects. Additionally, we carried out some attenuation measurements at GHz frequencies in liquid ^{4}He, since these measurements served two purposes: First, since our method is new, we wanted to test it with a relatively well-understood substance. Second, these measurements represent an extension of previous experiments[37,42] to higher frequencies. Before the experimental results in liquid and solid ^{4}He are presented and discussed in Sections 4 and 5, we summarize the theoretical background in Section 2 and describe the experimental setup in Section 3.

2. THEORETICAL BACKGROUND

Two different physical pictures have been used to describe the ultrasonic attenuation due to the interaction of a sound wave with thermal phonons: (a) In the approach of Landau and Rumer[13] the sound wave is regarded as a parallel beam of low-energy phonons. Because of anharmonic terms in the Hamiltonian of the crystal, interactions between different modes are possible and the rate at which the acoustic phonons are scattered is calculated by perturbation theory. (b) An alternative approach was first given by Akhieser.[16] Here, the sound wave is regarded as a macroscopic strain field in the crystal. Since the thermal phonon frequencies depend on strain, the local thermal equilibrium is disturbed. The tendency of the phonons to reestablish the thermal equilibrium by phonon interactions is a dissipative process. The response of the phonon system to the sound wave is calculated by means of the phonon Boltzmann equation. Maris[14] has given an extensive review of both methods. He showed that both approaches lead to identical results in the regime $1/\tau_{\text{th}} \ll \Omega \ll k_B T/\hbar$. If $\Omega\tau_{\text{th}}$ is not much greater than 1, the Akhieser approach should be used, while for $\Omega \approx k_B T/\hbar$, Landau–Rumer theory should be applied.[14]

For our measurements in solid helium $1/\tau_{\text{th}} < \Omega < k_B T/\hbar$ holds, so Landau–Rumer theory is more appropriate. The most important 3PP for the attenuation of longitudinal ultrasonic waves is L + L → L, where L denotes a longitudinal phonon. The inverse lifetime of the ultrasonic phonons $1/\tau$ due to this process, which is related to the amplitude attenuation coefficient α by $1/\tau = 2\alpha s$, has been shown to be[14]

$$\frac{1}{\tau} = \frac{\hbar^2\Omega^2}{\rho s^2 k_B T} \int_{k_1=0}^{\infty} \int_{\theta_1=0}^{\pi} \int_{\phi_1=0}^{2\pi} \gamma_s^2 \Omega_1^2 n_1(n_1+1) \times \frac{\tau_1 k_1^2\, dk_1\, d(\cos\theta_1) d\phi_1}{1 + \Omega^2\tau_1^2[1 - v_1(\cos\theta_1')/s]^2} \tag{1}$$

Here the index 1 refers to the thermal phonon, ρ is the density, s is the longitudinal sound velocity, and $n_1 = 1/[\exp(\hbar\Omega_1/k_B T) - 1]$ is the occupation number of thermal phonons. The wave vector $\mathbf{k}_1$ and the group velocity $\mathbf{v}_1$ of the thermal phonons are assumed to have the coordinates (k_1, θ_1, ϕ_1) and $(v_1, \theta_1', \phi_1')$ relative to the wave vector $\mathbf{k}$ of the sound phonon. $\gamma_s(k_1, \theta_1, \phi_1)$ is an effective Grüneisen parameter:

$$\gamma_s = -\sum_{\alpha\beta\gamma\delta\varepsilon\zeta} e_\alpha \hat{k}_\beta e_\gamma \hat{k}_\delta e_\varepsilon \hat{k}_\zeta (C_{\alpha\beta\gamma\delta\varepsilon\zeta} + C_{\alpha\beta\delta\zeta}\delta_{\gamma\varepsilon} + C_{\gamma\delta\zeta\beta}\delta_{\alpha\varepsilon} + C_{\varepsilon\zeta\beta\delta}\delta_{\alpha\gamma})/2\rho s^2 \qquad (2)$$

e_α are the components of the polarization vector of one of the three interacting phonons and $\hat{k}_\beta$ are the components of a unit vector in the direction of its wave vector. $C_{\alpha\beta\gamma\delta}$ and $C_{\alpha\beta\gamma\delta\varepsilon\zeta}$ are second- and third-order elastic constants, respectively. The term $\tau_1/\{1 + \Omega^2\tau_1^2[1 - v_1(\cos\theta_1')/s]^2\}$ in Eq. (1) ensures that only collisions that conserve momentum and energy within the energy uncertainty of the thermal phonons are included. Since $v_1 \approx s$ for the L + L → L process, the main contribution in Eq. (1) comes from nearly collinear 3PP, and therefore the angular dependence of the Grüneisen parameter and of the thermal phonon lifetime τ_1 can be neglected. If we first disregard the effect of anisotropy by setting $\theta_1' = \theta_1$, the angular integration can be performed:

$$\frac{1}{\tau} = \frac{2\pi\hbar^2\Omega}{\rho s k_B T}\int_{k_1=0}^{\infty} \gamma_s^2 \frac{\Omega_1^2 n_1(n_1+1)}{v_1} \times \left\{\tan^{-1}\left[\Omega\tau_1\left(1 + \frac{v_1}{s}\right)\right] - \tan^{-1}\left[\Omega\tau_1\left(1 - \frac{v_1}{s}\right)\right]\right\} k_1^2\, dk_1 \qquad (3)$$

To evaluate the integral over k_1, the dependence of γ_s on k_1 and the difference between v_1 and s is neglected except for the dispersion parameter $r_1 = (s - v_1)/s$. If one additionally assumes that τ_1 and r_1 in the $\tan^{-1}$ functions can be replaced by their values τ_{th} and r at $\bar{k}_1 = 4k_B T/\hbar s$, where the remaining part of the integrand has approximately its maximum, one obtains

$$\frac{1}{\tau} = \frac{\pi^2\hbar\Omega}{15\rho s^5}\gamma_s^2\left(\frac{k_B T}{\hbar}\right)^4 [\tan^{-1}(2\Omega\tau_{th}) - \tan^{-1}(r\Omega\tau_{th})] \quad \text{for} \quad \Omega\tau_{th} \gg 1 \qquad (4)$$

In the temperature regime where the relation $|r\Omega\tau_{th}| \ll 1 \ll \Omega\tau_{th}$ holds the second $\tan^{-1}$ function can be neglected while the first one is $\pi/2$, so we get the typical ΩT^4 law of the Landau–Rumer theory. At very low temperatures ($|r\Omega\tau_{th}| \gg 1$), $1/\tau$ is influenced by phonon dispersion. For normal dispersion ($r > 0$) both $\tan^{-1}$ terms in Eq. (4) almost cancel, leading to a stronger temperature dependence than T^4. However, if the dispersion is anomalous ($r < 0$), both terms are added, leading to a T^4 dependence of the attenuation with twice the prefactor as for $|r\Omega\tau_{th}| \ll 1$.

By setting $\theta_1' = \theta_1$ in Eq. (1) we have neglected the crystalline anisotropy. As was shown by Barrett,[17] this effect can be included in Eq. (4) by a dimensionless factor b for the principal directions of a crystal. For example, we obtain $b_a = 1.2$ for sound propagation in the direction of the a axis and $b_c = 2.5$ for the c axis of a hcp ^{4}He crystal, if we use the available elastic data.[2–4]

Finally we want to mention that sometimes the L + T → T process is more important for the attenuation of longitudinal waves than the L + L → L process. The attenuation due to this process, which is calculated in a similar way,[14] is proportional to T^4/τ_{th} for $\Omega\tau_{th} \gg 1$ and therefore proportional to T^9, since $1/\tau_{th}$ varies typically proportional to T^5 in good quality dielectric crystals.

In liquid ^{4}He the attenuation of sound waves can be calculated in a similar way as in dielectric crystals.[15] However, the relaxation times of the thermal excitations, i.e., phonons and rotons, are usually short ($\Omega\tau_{th} \lesssim 1$), so that the Akhieser approach is often used to calculate the sound attenuation. The difficulty in such a calculation is to account properly for the thermal relaxation times, which are determined by the various scattering processes between the thermal excitations. The situation is simpler in pure liquid ^{4}He *below* 0.6 K because only longitudinal phonons are present as thermal excitations. Then the Akhieser approach using a single relaxation time leads in the high-frequency limit ($\Omega\tau_{th} \gg 1$) to the same result as Landau–Rumer theory, Eq. (4) with $\gamma_s = u + 1$, where $u = (\rho/s)(\partial s/\partial \rho)$.[15] For $\Omega\tau_{th}$ not much greater than 1 some improvement has been achieved by Maris[18] regarding the choice of τ_{th}. He assumes that τ_{th} is determined below 0.6 K by 3PP which are allowed because of anomalous phonon dispersion. Since these are nearly collinear processes, phonons with different propagation directions can only interact by many 3PP. Then the reestablishment of thermal equilibrium between phonons of two given directions depends on the angle between them and therefore cannot be characterized very well by one relaxation time. Going beyond the single relaxation time approximation, Maris obtains good agreement with ultrasonic experiments and a measurement of the normal fluid viscosity.[18]

Above 0.6 K the rotons must also be taken into account. Khalatnikov and Chernikova[19,20] have studied this problem and Matveyev[21] has included the effect of anomalous phonon dispersion. They first investigate by which scattering processes thermal equilibrium is attained in the gas of elementary excitations, and find that roton–roton scattering and collinear phonon–phonon scattering guarantee a rapid establishment of equilibrium in the roton gas and in the phonon gas of a given direction. In comparison to these relaxation times, the phonon–roton relaxation time τ_{PR}—in which thermal equilibrium between both gases is attained—is very long. This slow re-

establishment of thermal equilibrium leads to appreciable sound absorption, which has a typical relaxation peak for $\Omega\tau_{PR} = 1$. At low temperatures, $\Omega\tau_{PR} \gg 1$, the expression for the sound attenuation transforms into Eq. (4), while for $\Omega\tau_{PR} \ll 1$ the hydrodynamic approximation[22] is obtained:

$$1/\tau = (\Omega^2/\rho s^2)(\tfrac{4}{3}\eta_n + \zeta_2) \tag{5}$$

where η_n and ζ_2 are the first and second viscosity coefficients. Above 1.2 K, Khalatnikov and Chernikova correct their calculation because τ_{PR} becomes comparable with the relaxation time in the phonon and roton gas itself.[19,20]

The sound wave also disturbs the thermal equilibrium of the roton gas, since the roton energy depends on density, too. This leads to additional absorption. Jäckle and Kehr have calculated this contribution with a Boltzmann equation approach.[23] They obtain in a relaxation time approximation for the attenuation

$$\frac{1}{\tau} = \frac{\Omega^2}{\rho s^2} \frac{3\eta_R}{1 + (\Omega\tau_{RR})^2} \tag{6}$$

Here η_R is the roton part of the viscosity and τ_{RR} the roton–roton collision time. Since η_R is nearly temperature independent, this contribution is temperature independent at high temperatures ($\Omega\tau_{RR} \ll 1$) and falls off proportional to $1/\tau_{RR}^2 \propto \exp(-2\Delta/k_B T)$ at low temperatures, where Δ is the roton energy.

3. EXPERIMENT

3.1. The Optical Arrangement

At first sight, the conventional ultrasonic technique using transducers seems to be the most appropriate method for attenuation measurements. This method has been successfully used to determine the sound velocities in both liquid and solid ^{4}He.[15] Attenuation measurements in solid ^{4}He with conventional ultrasonics, however, are hindered by several parasitic attenuation effects so that no reliable results have been obtained until now. The dominant source of spurious attenuation comes from nonparallelism of the reflecting surfaces, which introduces phase differences of the acoustic signal on the receiving transducer and leads to interference effects. These interference effects, which are already difficult to circumvent in liquid helium, appear to be still more severe in solid helium because of the acoustical anisotropy and imperfections in growing high-quality single crystals over the whole chamber volume.

In our experiment we used an optical technique which avoids these difficulties. The sound wave was generated in the medium by stimulated

Brillouin scattering (SBS) using a giant pulse ruby laser.[24] While the intensive light beam is scattered in the backward direction in this process, the sound is propagating in the direction of the incident light. Only longitudinal phonons are generated by SBS, which have a wavelength of

$$\lambda_S = \lambda_L/2n \tag{7}$$

where λ_L is the wavelength of the laser light ($\lambda_L = 6943$ Å for a ruby laser) and n is the refractive index of the sample. The backscattered Brillouin light has a frequency shift $\Delta\nu$ with respect to the incident light which is equal to the phonon frequency $\Omega/2\pi$:

$$\Delta\nu = \Omega/2\pi = 2ns/\lambda_L \tag{8}$$

According to the strongly pressure-dependent sound velocity s in condensed helium, the frequency shifts vary considerably and are of the order of 0.7 GHz in liquid ^{4}He at svp and 1.5 GHz in hcp ^{4}He at 36 bar.

The sound velocity in hcp ^{4}He also depends on the crystal orientation. Therefore we have measured the frequency shift $\Delta\nu$, which is connected with the sound velocity by (8), to get some information about the crystal orientation. Since it is difficult to resolve these small shifts with sufficient

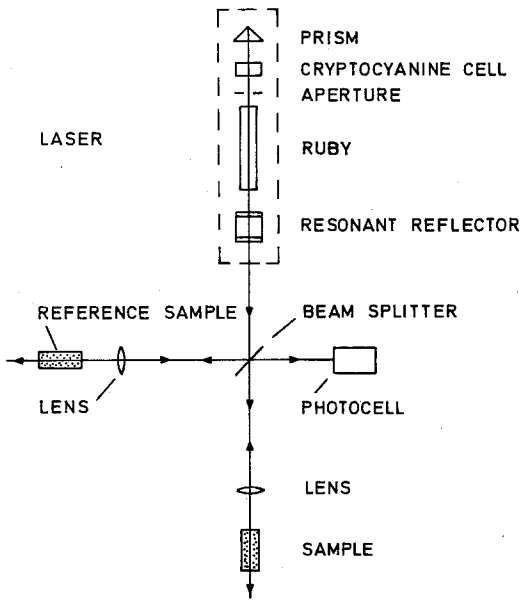

Fig. 1. Experimental setup for measuring phonon velocities by stimulated Brillouin scattering.

accuracy by a Fabry-Perot interferometer, we used an optical heterodyne method.[25] The experimental setup is shown in Fig. 1. The light beam of the single-mode ruby laser, which is passively Q-switched, is split into two parts by a beam splitter. The transmitted part of the light is focused into the sample, the reflected part into the reference sample. Since both substances have an equal distance from the laser, SBS simultaneously develops in both materials. The backscattered light beams, which have a frequency difference of

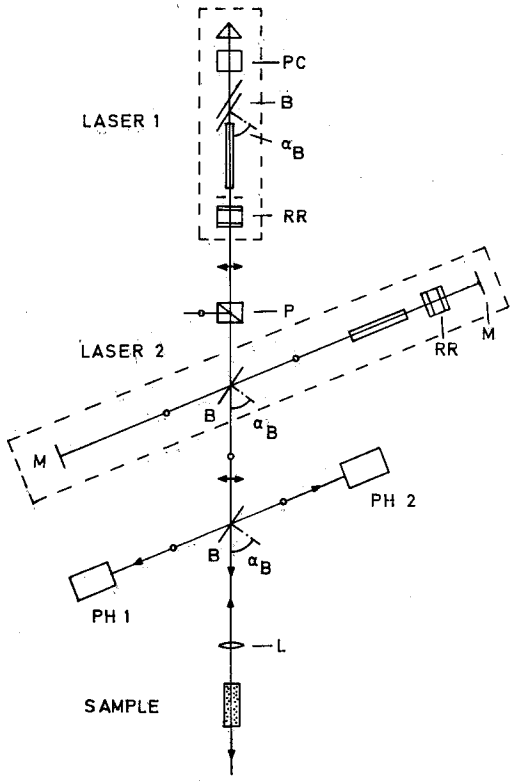

Fig. 2. Experimental setup for measuring phonon lifetimes by stimulated Brillouin scattering. The giant pulse ruby laser 1 is Q-switched by a Pockels cell PC. Its polarization is in the plane of the paper. The polarization of ruby laser 2 is perpendicular to it (indicated by circles). Resonant reflectors RR are used for mode selection. Photocells PH 1 and PH 2 record incident and backscattered light of laser 2. Registration of laser 1 is strongly suppressed, because the beam splitter B is mounted at the Brewster angle.

$2(n_1 s_1 - n_2 s_2)/\lambda_L$ with respect to one another, generate a beat signal on the photocell (TRG 105B) which is recorded by an oscilloscope (Tektronix 519). As reference substance we chose N_2 gas at 100 bar, which has a low threshold for SBS and for which $\Delta\nu = 1.1$ GHz. The method was tested with liquid ^{4}He at svp giving a sound velocity which was in agreement within the experimental uncertainty of 1% with other data.[26]

In order to determine the attenuation of the longitudinal sound wave generated by SBS, we used a method which is an improvement of the "two-pulse method" used by Winterling and Heinicke.[27] The experimental setup is shown schematically in Fig. 2. We want to describe here only the principle of measurement. A more detailed account of the method has already been given.[28] Ruby laser 1 generates the phonons by SBS and light from a second ruby laser, laser 2, which is directed into the light path of laser 1 by a beam splitter, is used as test light. After generation of the ultrasonic phonons by laser 1 the test light of laser 2 is now scattered back by these phonons. If the test light intensity is sufficiently weak that it does not disturb the phonon distribution, the backscattered intensity is proportional to the number of the phonons still present. As the phonons decay, the backscattered intensity decreases with time. Thus from the time-dependent ratio of the backscattered light power P_2 to the incident light power P_1 the absolute value of the phonon lifetime can be obtained. The accuracy of the method is approximately 10%.

In Fig. 3 the ratio P_2/P_1 as obtained in some typical experiments is plotted as a function of time on a semilogarithmic scale. The straight line of the curve for ^{4}He at svp and 0.64 K indicates that the sound intensity decreases exponentially. At lower temperatures, however, a nonexponential decrease of P_2/P_1 and therefore of the sound intensity was observed, indicating that finite amplitude effects influenced sound attenuation. The nonexponential decay appeared in liquid ^{4}He at svp below 0.6 K, in liquid ^{4}He at 23 bar at 0.8 K, and in hcp ^{4}He at 36 bar below 1.3 K. As is shown in Fig. 3, the $\log(P_2/P_1)$ plot was characterized in this case by a short decay time τ' just after phonon generation and a long decay time τ'' at the end of the observation time interval. The time τ' was temperature independent but varied roughly inversely proportional to the amplitude of the sound wave, which could be changed within a factor of three by varying the intensity of laser 1. At the highest accessible light intensities when saturation occurred in SBS[24] a nearly constant τ' was observed, which was 300 nsec in liquid ^{4}He at svp and 80 nsec in solid ^{4}He at 36 bar. This is consistent with a constant sound amplitude in the saturation regime of SBS, which we estimate to be $(\Delta\rho/\rho)_0 = 5 \times 10^{-4}$ in both liquid and solid ^{4}He.

The most likely process which causes a nonexponential decay is the generation of higher harmonics in the sound wave, which leads to shock wave formation. A sound wave transforms to a shock wave in a nonviscous

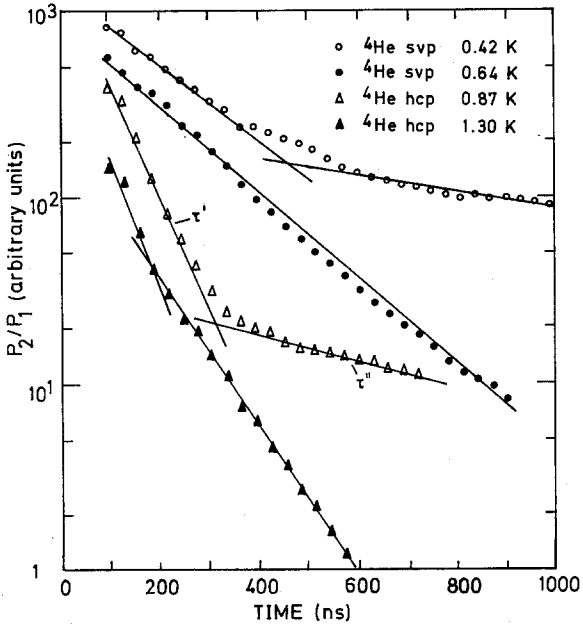

Fig. 3. Ratio of backscattered to incident light power P_2/P_1 as a function of time at two temperatures in liquid ^{4}He at svp and hcp ^{4}He at 36 bar. Straight lines indicate an exponential decrease of P_2/P_1.

liquid within a time interval[29]

$$t_s = \frac{1}{s(u+1)k(\Delta\rho/\rho)_0} \tag{9}$$

where $u = (\rho/s)(\partial s/\partial\rho)$, k is the wave vector of the sound wave, and $(\Delta\rho/\rho)_0$ is the initial sound amplitude. [Since the generation of the higher harmonics can be considered as a 3PP, Eq. (9) may be generalized to solids if $u + 1$ is replaced by the generalized Grüneisen parameter defined by Eq. (2).[30]] Blackstock[31] has considered the propagation of a finite amplitude wave in a nonviscous fluid, and from this work we estimate that the intensity of the first harmonic, which is observed in this experiment, falls off with a mean decay time of $\tau_{\text{fin}} \approx 2t_s$ in a time period of the order of $5t_s$ after generation of the sound wave. In liquid ^{4}He at svp (where $u = 2.84, k = 1.86 \times 10^5$ cm^{-1}, and $s = 2.4 \times 10^4$ cm/sec) we get from (9) $\tau_{\text{fin}} = 2t_s = 240$ nsec for $(\Delta\rho/\rho)_0 = 5 \times 10^{-4}$. This is in reasonable agreement with the experimentally determined value of $\tau' = 300$ nsec in the saturation regime of SBS, which confirms the assumption of shock wave formation. If we accept this to be also true for

solid ^{4}He, we can also estimate the effective anharmonicity from the experimental value τ'. We will investigate this point further together with the discussion of the attenuation measurements in Section 5.

In order to get the phonon lifetime for small sound amplitude we proceeded as follows: If the ratio of the backscattered to incident light power decreased exponentially and there was no variation of the decay time with the initial sound amplitude $(\Delta\rho/\rho)_0$, which could be reduced by a factor three, we took this decay time as the true phonon lifetime. In this way all the data presented in this paper for liquid helium and those for solid ^{4}He at 36 bar above 1.3 K were determined. The data for solid ^{4}He below 1.3 K were partially taken from exponential (P_2/P_1) curves, which were recorded at low sound amplitudes, and partially from the exponentially decaying tail (τ'' in Fig. 3) of nonexponential curves. This method of data reduction has given reproducible results in solid ^{4}He down to 0.8 K.

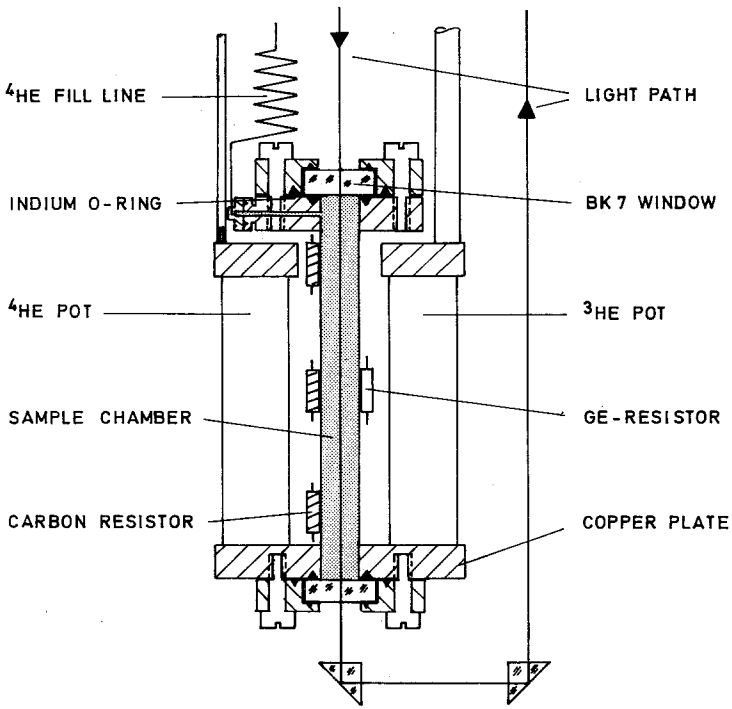

Fig. 4. Sample chamber assembly.

3.2. The Cryostat

The cryostat for growing ^{4}He crystals was similar to those used in the thermal conductivity measurements of Hogan *et al.*[32] and Berman *et al.*[33] As has been reported, high-quality crystals have been obtained in these experiments. The sample chamber assembly is shown in Fig. 4. Temperatures down to 0.4 K were obtained by pumping ^{3}He which was inside the ^{3}He pot. Another pot, referred to as ^{4}He pot, which was filled with liquid ^{4}He, was used for crystal growth. The sample chamber, an 80-mm-long, 10-mm-ID stainless steel tube, was hard-soldered between these pots to a common copper plate. The sample chamber was closed on both ends by 8-mm-thick windows made of BK 7 glass. The windows were sealed at both surfaces by indium O-rings. This method of sealing was vacuum-tight and produced negligible induced stress birefringence up to 100 bar. The cell was filled with 99.9 % clean ^{4}He gas from a high pressure cylinder via a N_2 cold trap and a 0.4-mm-ID capillary.

The crystals were grown at constant pressure of 36 bar by lowering the temperature of the bottom of the sample chamber 0.1 K below the melting temperature $T_M = 1.95$ K. After a crystal had formed on the lower window the temperature was reduced by 0.2 K and slowly lowered to 1.2 K when the freezing surface had reached the middle of the cell. The outer ^{4}He bath was well above the melting temperature to guarantee an open fill line during crystal growth. The growth rate was approximately 4 cm/h.

The experiments with liquid ^{4}He were carried out in the same cryostat but only temperatures of 0.65 K were reached because of the large heat input through the fill line. Therefore the method reported by Abraham *et al.*[34] was used for the measurements below 0.65 K.

4. RESULTS AND DISCUSSION: LIQUID ^{4}He

4.1. Liquid ^{4}He at svp

We have measured the phonon lifetimes with the method described in Section 3 in superfluid ^{4}He at svp between 0.4 K and T_λ. The ultrasonic attenuation in this substance has already been determined for several frequencies,[15] and therefore this experiment provided a good test for our optical method. In addition, we have obtained results in a frequency and temperature regime which so far has not been accessible by other methods. The wave vector of the longitudinal phonons generated by SBS is $k = 1.859 \times 10^5$ cm^{-1} in liquid ^{4}He at svp, and therefore the frequency $\Omega/2\pi = sk/2\pi$ is 0.705 GHz at low temperatures, where $s = 2.383 \times 10^4$ cm/sec.[35] Since s is temperature dependent, the frequency decreases by about 4 % between 1 and 2 K.

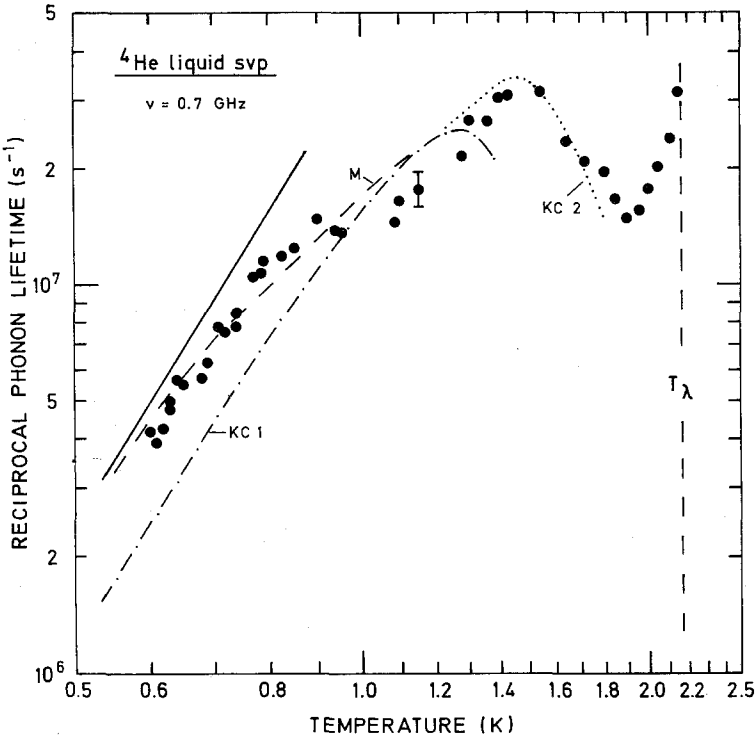

Fig. 5. Reciprocal phonon lifetime in liquid ^{4}He at svp as a function of temperature at a frequency of 0.7 GHz. The data points are compared with several theoretical works: (– · –) KC 1, theory of Khalatnikov and Chernikova below 1.2 K.[19,20] (· · ·) KC 2, theory of Khalatnikov and Chernikova above 1.2 K calculated for 723 MHz by Hohenberg and Platzman[38] (scaled to 705 MHz by an Ω extrapolation below 1.5 K and by an Ω^2 extrapolation above). (– – –) M, theoretical curve after work of Matveyev.[21] (—) limit for the 3PP in the case of anomalous dispersion [Eq. (4)].

We only present here the data above 0.6 K, where an exponential decrease of the phonons has been observed. In Fig. 5 the measured inverse phonon lifetimes are plotted as a function of temperature. The strong increase of the attenuation at T_λ is closely related to the properties of a second-order phase transition and has already been discussed extensively.[15,36] On decreasing the temperature, the characteristic phonon roton relaxation peak is reached at 1.45 K. For $T > T_{\text{peak}}$ where $\Omega\tau_{\text{PR}} \ll 1$ holds we can compare our measurements with the ultrasonic experiments of Abraham *et al.*[37] by scaling their data at 30 MHz by an Ω^2 extrapolation according to Eq. (5) to 705 MHz. The two results agree within 10 %. St. Peters *et al.*[26] have determined the attenuation in ^{4}He at svp by measuring the linewidth

in a *spontaneous* Brillouin scattering experiment at a wave vector $k = 2.033 \times 10^5\ \mathrm{cm}^{-1}$, which is nearly the same as in our experiment. If we scale these data in the region of the relaxation maximum by a linear extrapolation to our wave vector assuming a linear Ω dependence as in Landau–Rumer theory, we again get agreement within 10%.

Between 0.6 and 1 K these are the first measurements at such high frequencies. As apparent from Fig. 5, the attenuation does not simply fall off at the low-temperature side of the relaxation peak, but a shoulder appears between 0.8 and 1 K. A fit to the data below the shoulder gives for the inverse phonon lifetime

$$1/\tau = 2.6 \times 10^7 T^{3.7 \pm 0.3} \quad \mathrm{sec}^{-1} \tag{10}$$

Since both this experiment and the ultrasonic measurements of Abraham *et al.* at 204 MHz[37] show approximately a T^4 dependence at low temperatures, we can assume that the attenuation is caused by the 3PP in both cases. Then we can scale the data of Abraham *et al.* at 204 MHz between 0.1 and 0.35 K according to (4) by an Ω extrapolation to 705 MHz and get $1/\tau = 3.9 \times 10^7\ T^{4,3}\ \mathrm{sec}^{-1}$, which agrees with our data at 0.6 K within 10%.

Now we compare the data with the theory of Khalatnikov and Chernikova (KC).[19,20] An expression for the sound attenuation in the KC theory between 0.6 and 1.2 K is given in the work of Abraham *et al.*[37] Using the same phonon and roton parameters as in that work except for the Grüneisen parameter, for which we used the value 2.84,[35] we obtained for $1/\tau$ the curve KC 1 as shown in Fig. 5. For KC theory above 1.2 K and at high frequencies ($\Omega\tau_{\mathrm{th}} \gtrsim 1$) we used a previous calculation of Hohenberg and Platzman for 723 MHz,[38] which is shown in Fig. 5 by the curve KC 2. The agreement between KC 2 and the experimental data is good in the region of the relaxation peak and above, while below the maximum down to 1 K, KC 1 and KC 2 lie approximately 15% above the data.

This difference may arise from the choice of the Grüneisen parameter. Usually the Grüneisen constant for the thermal phonons is approximated by the Grüneisen constant of the acoustic phonons, which is deduced from the pressure dependence of the sound velocity at low temperatures.[35] Now it is assumed[18] that the dispersion curve in liquid ^{4}He is anomalously bent upward for small k vectors but turns down to normal dispersion above a certain cutoff wave vector k_c which is shifting in liquid ^{4}He to lower values with increasing pressure.[23] This may affect the Grüneisen parameter for the thermal phonons. Jäckle and Kehr[23] have specified the dispersion curves for different pressures and we have estimated from this work the following dependence of the Grüneisen constant on the wave vector k:

$$u_k = u_{k=0} - (k/k_c)^4 \qquad \text{for} \quad k < k_c \tag{11}$$

for ^{4}He at svp. For the dispersion curves of ^{4}He at svp specified by Jäckle and Kehr[23] or Maris[18] we get for the Grüneisen constant of $4k_BT$ thermal phonons a value of 2.6 for 1.1 K, which gives better agreement with the data when used in KC 1.

Below 1 K, where $\Omega\tau_{PR} \gg 1$ holds, the KC theory transforms into the result of the Landau–Rumer theory, Eq. (4), without dispersion ($r = 0$). In contrast to the experimental data, no shoulder appears in the KC theory in the vicinity of 0.8 K and the theoretical values lie a factor of 1.6 below the data. This difference, which already appears in the ultrasonic experiments at lower frequencies, indicates anomalous phonon dispersion as was first proposed by Maris and Massey.[40] However, a factor of two is expected from Eq. (4) if the anomalous dispersion is fully developed ($-r\Omega\tau_{th} \gg 1$), and the question arises why the experimental results indicate a smaller factor. Maris[18] has calculated the ultrasonic attenuation for ^{4}He at svp below 0.6 K without using a relaxation time approximation. A surprising result was that the attenuation can be more than a factor of two higher than that predicted from (4) for $r = 0$ because of the coupling of the sound wave to a second sound mode. This is the case for $\Omega\tau_{\|} \approx 1$, where $\tau_{\|} = 2 \times 10^{-10}$ T^{-5} sec is the relaxation time for the 3PP under small angle. For $\Omega\tau_{\|} \gg 1$ the attenuation agrees with the Landau–Rumer result for anomalous dispersion. Since $\Omega\tau_{\|} \approx 10$ holds for 700 MHz at 0.6 K, we should expect an attenuation which is a factor of two higher or slightly more, in contrast to experiment. The same deviation seems already to be present at lower temperatures in the ultrasonic experiments at lower frequencies, as is discussed in the work of Maris[18] and Wehner.[41] No satisfactory explanation has been given for this difference.

The temperature regime above 0.6 K is beyond the range of the theory of Maris[18] since phonon–roton scattering processes must be taken into account. In order to explain the shoulder, we therefore used the work of Matveyev,[21] who included the effect of anomalous phonon dispersion in the KC theory. However, we used the phonon dispersion curve C given by Maris[18] instead of that used by Matveyev, because Maris could explain the ultrasonic experiments of Abraham *et al.*[37] with this dispersion curve rather well. Therefore we have also considered 3PP above 0.6 K when estimating the thermal phonon relaxation time. The result of this calculation is shown in Fig. 5 by curve M. While the transition of the curve M to KC theory lies in the right temperature region of 0.8 K, a pronounced shoulder does not appear in M. The agreement may be improved if one takes into account that the approximations $u_k = u_0$ and $\varepsilon(k) = sk$ for the Grüneisen constant and the energy of the thermal phonons were made. But we also think it possible that k_c may be temperature dependent and shifts to smaller values above 0.6 K. This could provide an explanation for the shoulder equally well.

4.2. Liquid ^{4}He at 23 bar

The ultrasonic experiments of Roach *et al.*[42] have shown that in liquid ^{4}He under pressure the ultrasonic attenuation due to the 3PP is strongly reduced because of normal dispersion. This reduction is very pronounced in the neighborhood of the melting curve. Since one intention of our sound absorption measurements in solid ^{4}He was to investigate the phonon dispersion, we also measured the sound attenuation in liquid ^{4}He at 23 bar, to be able to make a comparison between the liquid and the solid in this respect. The wave vector of the longitudinal phonons generated by SBS is

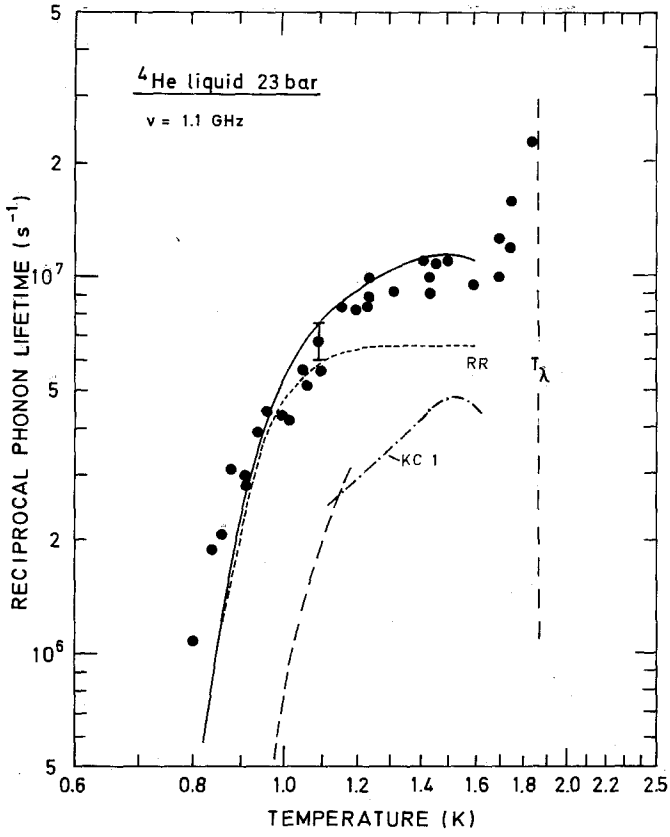

Fig. 6. Reciprocal phonon lifetime in liquid ^{4}He at 23 bar as a function of temperature at a frequency of 1.1 GHz. (– – –) Landau–Rumer theory for normal phonon dispersion [Eq. (4)]. (– · –) KC 1, theory of Khalatnikov and Chernikova.[19,20] (– – –) RR, attenuation due to roton–roton relaxation [Eq. (6)]. (—) Sum of all contributions to the attenuation.

in this case $k = 1.87 \times 10^5$ cm^{-1} and the frequency is 1.1 GHz for $s = 3.6 \times 10^4$ cm/sec.[35]

The experimental results for the inverse phonon lifetime $1/\tau$ in the temperature regime between 0.8 K and T_λ are shown in Fig. 6. The attenuation sharply increases at T_λ as in ^{4}He at svp, but the relaxation peak in the neighborhood of 1.4 K has transformed into a broad shoulder. Below 1.2 K the attenuation is falling off stronger than T^4, which seems to be an indication for normal dispersion. For a quantitative comparison Landau–Rumer theory, Eq. (4), was used at low temperatures. A dispersion parameter $r = 3\bar{\gamma}k^2 = 2.1 \times 10^{-2} T^2$ was obtained by assuming thermal phonons of energy $4k_B T$ and a phonon dispersion curve of the form $\Omega = sk(1 - \bar{\gamma}k^2)$. The value $\bar{\gamma} = 0.69$ Å^2 was taken from the neutron scattering experiments of Svennson *et al.*[43] We have estimated the lifetime of 4 $k_B T$ thermal phonons, which above 0.8 K is mainly determined by phonon–roton scattering, by using the expression for $1/\tau_{PR}(k)$ given in the work of Khalatnikov and Chernikova.[19,20] The roton parameters were taken from the neutron scattering experiment of Dietrich *et al.*[44] at 1.3 K. The calculation of the thermal phonon lifetime shows that above 1.2 K the relation $\Omega\tau_{th} \gg 1$ is no longer valid. Above this temperature we therefore applied the KC 1 theory of Khalatnikov and Chernikova.[19,20] In Fig. 6 the prediction from Landau–Rumer theory is shown by a dashed line while KC theory is indicated by a dashed-dotted line.

Apparently the attenuation is much larger than estimated. This additional attenuation is produced by roton–roton relaxation.[23] Such a contribution can be neglected in ^{4}He at svp but not in the liquid under pressure, because the roton energy decreases and the phonon energy at a given wave vector increases with pressure, thus raising the roton contribution to the thermal excitations. We have calculated the roton–roton relaxation process according to Eq. (6). The roton viscosity $\eta_R = 11\ \mu$P was taken from the experiment of Brewer and Edwards,[39] and for the roton–roton relaxation time $\tau_{RR} = 1 \times 10^{-13}\ T^{-1/2} \exp(7.1/T)$ was used.[23] The result is shown in Fig. 6 by the dashed line RR. If we add all contributions, we get the solid line in Fig. 6, which is in reasonable agreement with experiment between 1.0 and 1.6 K.

Below 1.0 K the data lie somewhat above the theoretical prediction. This extra absorption may arise from an interaction between the ultrasonic phonons and rotons where the acoustic phonon is absorbed by a roton to produce another roton of higher energy. This process, which was first suggested by Pitaevskii,[45] is allowed if the group velocity of the rotons becomes equal to the sound velocity. Jäckle and Kehr[46] have calculated the ultrasonic attenuation due to this process in the high-frequency limit ($\Omega\tau_{RR} > 1$). From this work we estimate for our experiment $1/\tau = 6 \times 10^5$

sec^{-1} for $T = 0.9$ K, which has the right order of magnitude to explain the extra attenuation. (Unfortunately, $\Omega\tau_{RR}$ approaches 1 in this temperature regime and so it is questionable to apply the work of Jäckle and Kehr.) In summary, our results show that for $T > 0.8$ K the ultrasonic attenuation in ^{4}He at 23 bar is mainly determined by the interaction of the sound wave with the roton gas. The 3PP only plays a minor role in this substance.

5. RESULTS AND DISCUSSION: SOLID ^{4}He

5.1. Results

Hcp ^{4}He crystals were grown at a pressure of 36 bar, corresponding to a melting temperature of 1.95 K and a molar volume of 20.3 cm^3. For this molar volume thermal conductivity[32,33] as well as sound velocity measurements[2–4] have been reported. We have estimated the lifetime of the thermal phonons from the thermal conductivity measurements of Berman *et al.*[33] in hcp ^{4}He at 39 bar and found that below the melting point the relation $\Omega\tau_{th} > 1$ holds for longitudinal phonons in the GHz regime, so that Landau–Rumer theory should apply. Equation (4) implies that in Landau–Rumer theory the attenuation strongly depends on the sound velocity. Since the sound velocity in hcp ^{4}He varies appreciably with the orientation of the crystal,[4] we have measured the velocity of the longitudinal phonons with the method described in Section 3. This also provided an estimate for the crystal orientation, from the known orientation dependence of the sound velocity.[4]

The measurement of the phonon lifetimes in hcp ^{4}He was more difficult than in liquid ^{4}He. For example, the polarization of laser 1 had to be parallel to the slow or the fast axis of the birefringent hcp crystal, since otherwise the backscattered light of laser 1 could not be suppressed by the polarization optics as described in a previous paper.[28] Another difficulty was that the backscattered light of the probing light pulse was modulated in some crystals. We attribute this effect, which has never been observed in liquid ^{4}He, to crystalline grains in the focal volume with slightly different orientations. Due to the orientation dependence of the sound velocity, the backscattered light signals have different frequency shifts and thus are generating a beat note. The oscillations had a period of the order of 100 nsec, which corresponds to $\Delta s/s \approx 0.5\%$. In one crystal, however, both difficulties did not appear. The measured sound velocity was 500 ± 10 m/sec in this case. The frequency of the longitudinal phonons with wave vector $k = 1.87 \times 10^5$ cm^{-1} is then 1.50 GHz. In a hcp crystal the sound velocity only depends on the angle θ between the propagation direction and the c axis. If we use the data of Greywall[4] for $s(\theta)$, we can conclude $40° \leq \theta \leq 90°$ for our experiment. Greywall has reported that the hcp ^{4}He crystals preferentially grow with

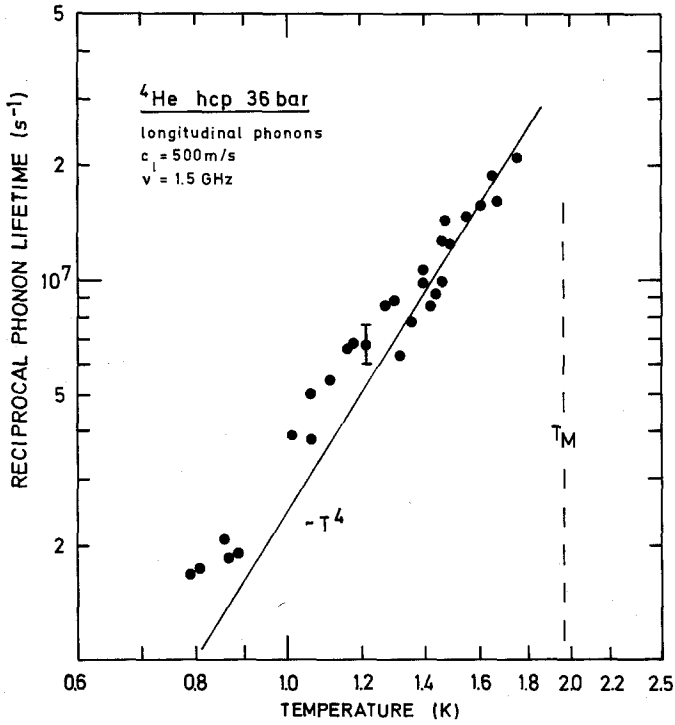

Fig. 7. Reciprocal lifetime for longitudinal phonons at a frequency of 1.5 GHz in hcp ^{4}He at 36 bar as a function of temperature. T_M denotes the melting temperature. The solid line indicates the expected T^4 temperature dependence after Eq. (4) for $r = 0$.

the c axis nearly parallel to the freezing surface. This observation would indicate that the phonons propagate in our experiment parallel to the basal plane ($\theta = 90°$).

The phonon lifetimes were determined in solid helium between 0.8 and 1.7 K as described in Section 3. In Fig. 7 the measured reciprocal phonon lifetimes $1/\tau$ are shown as a function of temperature. Above 1.3 K, where an exponential decrease of the phonons was observed, the inverse phonon lifetime follows the relation

$$1/\tau = 2.8 \times 10^6 T^{3.6} \quad \text{sec}^{-1} \tag{12}$$

and therefore is approximately proportional to T^4. A similar temperature dependence was observed below 1.3 K, but with a prefactor which is 25% higher. This could be interpreted as a shoulder between 1.2 and 1.4 K which leads to an overall temperature dependence which is smaller than T^4.

Similar but not so extensive results were obtained in several other hcp crystals grown at 36 bar.*

5.2. Comparison with Landau–Rumer Theory (Dispersionless Case)

First we discuss the results in the temperature range above 1.3 K. The T^4 dependence indicates that the 3PP $L + L_{th} \rightarrow L_{th}$ is responsible for the attenuation, and therefore Eq. (4) may be used. We neglect the influence of phonon dispersion ($r = 0$) and assume for the anisotropy parameter $b = b_a = 1.2$, which means sound propagation in the basal plane. Taking the effective Grüneisen parameter γ_s as an adjustable parameter, we get agreement between Landau–Rumer theory and experiment for $\gamma_s = 6.9$. As we have already mentioned in Section 3, an estimate for γ_s can also be obtained by comparing the shock time in liquid ^{4}He at svp with that of solid ^{4}He by means of Eq. (9). We have estimated the amplitude of the sound wave $(\Delta\rho/\rho)_0$ in solid ^{4}He to be the same as in the liquid in the saturation regime of SBS. The shock times in ^{4}He at svp and in hcp ^{4}He at 36 bar were 150 and 40 nsec, respectively, so we get $\gamma_s = 6.8$ from Eq. (9), which compares quite well with γ_s obtained above.

This effective Grüneisen parameter is considerably larger than that in liquid ^{4}He ($\gamma_s = 3.84$ at svp and $\gamma_s = 3.23$ at 23 bar[35]) and also exceeds the thermal Grüneisen constant $\gamma_{cal} = 2.7$ in hcp ^{4}He[48] by a factor of 2.5. Although γ_s and γ_{cal} are different quantities, this large difference is surprising and therefore it is interesting to make an estimate for γ_s. Jäckle and Kehr[12] have predicted that the effective anharmonicity γ_s of a quantum solid is determined as in normal dielectric crystals, and therefore Eq. (2) holds. If we assume that the sound wave is propagating along the (100) direction, then we get $\gamma_s = -(C_{111} + 3C_{11})/2C_{11}$. Taking $C_{11} = 0.5$ kbar for our experiment,[4] we obtain $C_{111} = -8.4$ kbar. Now this value can be compared with C_{111} determined from the dependence of the elastic constants from uniaxial and hydrostatic pressure. Using the work of Brugger,[49] we can express the density dependence of C_{11} on hydrostatic pressure by

$$C_{111} + C_{112} + C_{113} = -2C_{11}(3U_{11} + 2) - 3/K = -11.0 \text{ kbar} \qquad (13)$$

where the compressibility K was chosen to be 3.1 kbar^{-1},[55] and

$$U_{11} = \tfrac{1}{2}\partial[\ln(C_{11}/\rho)]/\partial(\ln\rho) = 2.7 \pm 0.1$$

*We have already reported on some attenuation measurements which show a weaker temperature dependence than the results presented here.[47] In these previous experiments, which were carried out in the temperature regime above 1.2 K, finite amplitude effects could not be distinguished because the sensitivity of the photocells used was not high enough to observe the decrease of the phonons over a wide range of sound intensities. Therefore these results must be regarded as being influenced by finite amplitude effects.

was extracted from a fit to the available elastic data.[2–6] (We have omitted the distinction between the isothermal and the adiabatic elastic constants, since the differences are small in hcp ^{4}He. Besides, we have used the fact that the c/a ratio of hcp ^{4}He is pressure independent for the calculation of the compliances s_{ik} and the linear compressibilities β_a and β_c along the principal directions.[2]) In order to eliminate C_{112} and C_{113} from Eq. (13), we need the dependence of C_{11} on uniaxial pressure. Unfortunately, this quantity is not known for hcp ^{4}He. Therefore we assumed that the ratio of the C_{jkl}'s in hcp ^{4}He is the same as is given by an hcp crystal with nearest-neighbor central force interaction. Clearly this model is not well suited for a quantum crystal. But actually, the ratio of the second-order elastic constants of hcp ^{4}He does not deviate more than 20 % from the ratio predicted by this model. Since it is generally expected[50] that the third-order elastic constants follow this model much closer than the second-order elastic constant, this approximation may be allowed. Under this assumption we get the relations[51] $C_{111}:C_{112}:C_{113} = 247:85:16$. Using these relations, we obtain from Eq. (13) $C_{111} = -7.9$ kbar, which is in good agreement with the value quoted above. This estimate shows that hcp ^{4}He can indeed have such a large value for γ_s. However, we must regard this good agreement to be fortuitous since γ_s shows a large anisotropy, even within the basal plane. If we use the nearest-neighbor central force model to calculate γ_s from Eq. (2) for different directions, we find an anisotropy of up to 30 % for the orientation directions which are still possible from our sound velocity measurement. Therefore for a better experimental proof of the prediction of Jäckle and Kehr for γ_s in a quantum solid the crystal orientation must be determined more accurately, e.g., by x-ray scattering.[4]

5.3. Influence of Phonon Dispersion

A further intention of these experiments was to search for an influence of phonon dispersion on the 3PP. If we neglect that the data below 1.3 K lie somewhat above the T^4 extrapolation in Fig. 7, then the results indicate that dispersion does not play a role above 0.8 K. If we want to check this observation, we have to estimate the dispersion term $\tan^{-1}(r\Omega\tau_{th})$ in Eq. (4). In a linear chain model with nearest-neighbor interaction the phonon dispersion parameter for $4k_BT$ thermal phonons can be approximated by $r = (L^2/8)(4k_BT/\hbar s)^2$, where L is the interatomic distance.[14] If we use $L = a = 3.6 \times 10^{-8}$ cm for hcp ^{4}He at 36 bar,[5] we get $r(T) = 1.8 \times 10^{-2} T^2$, which is of the same order of magnitude as the experimentally determined value in liquid ^{4}He at 23 bar. The thermal phonon lifetime τ_{th}, which we also need for the estimate, is assumed to be determined by Umklapp processes with the relaxation time τ_U and by normal processes with the relaxation

time τ_N: $1/\tau_{th} = 1/\tau_U + 1/\tau_N$. For a first estimate $1/\tau_U$ may be taken from thermal conductivity measurements,[32,33] which give $1/\tau_U = 2 \times 10^{11} T^3 \times \exp(-11.2/T)$ for hcp ^{4}He at 36 bar. $1/\tau_N = 2 \times 10^7 T^3$ may be extracted from thermal conductivity experiments under Poiseuille flow conditions[32,33] and from second sound experiments.[52] However, if we estimate the dispersion term in Eq. (4) with these parameters, we expect already for $T = 1.6$ K a reduction of the 3PP and therefore a steeper temperature dependence than T^4, which is in contrast to experiment.

From our point of view this indicates that thermal conductivity measurements and second sound experiments which predominantly probe transverse phonons give a wrong estimate for the lifetime of the longitudinal thermal phonons which interact in the 3PP. Therefore we tried to estimate τ_{th} in another way. We assume that the lifetime for the longitudinal $4k_B T$ thermal phonons is mainly determined by phonon decay processes of the form $L \rightarrow T + T$, $L \rightarrow L + T$, and $L \rightarrow L - T$. Then we can use the work of Klemens[53,54] for an estimate of τ_{th} and find $1/\tau_{th} = 4 \times 10^8 T^5 \text{ sec}^{-1}$ assuming $\gamma = 3$ for the effective Grüneisen parameter. With this rough estimate we find that dispersion effects should play no role in the temperature range of our experiment. Therefore, the small lifetime of the longitudinal thermal phonons due to decay processes of the form $L \rightarrow L + T$ and $L \rightarrow T + T$ seems to be responsible for our failure to detect an influence of phonon dispersion on ultrasonic attenuation as in liquid ^{4}He at 23 bar.[42]

6. SUMMARY

The intention of this experiment was to study phonon–phonon interactions in the quantum crystal ^{4}He by measuring the temperature dependence of the ultrasonic attenuation. It is found that the attenuation of longitudinal 1.5-GHz phonons in hcp ^{4}He at 36 bar approximately shows a T^4 temperature dependence between 0.8 and 1.75 K. This temperature dependence, which has already been observed in many dielectric crystals, is typical for a three-phonon interaction of the ultrasonic phonons with longitudinal thermal phonons first considered by Landau and Rumer.

For a quantitative comparison with Landau–Rumer theory the third-order elastic constants of solid ^{4}He must be known. Assuming sound propagation along the (100) direction of the hcp crystal, the relevant constant C_{111} is estimated from the measured volume dependence C_{11} in a nearest-neighbor central force model. The attenuation calculated with Landau–Rumer theory under these assumptions is in satisfactory agreement with experiment, and therefore confirms the prediction of Jäckle and Kehr that the damping of the phonons in quantum crystals is dominated by three-phonon processes due to an effective anharmonicity which can be expressed by the third-order elastic constant as in normal dielectric crystals.

Additionally, the data indicate that the attenuation due to the 3PP is not affected by normal phonon dispersion down to 0.8 K. It is shown that this observation is compatible with a parameter for normal dispersion found in *liquid* ^{4}He at 23 bar and an estimate for the lifetime of thermal phonons due to decay processes of the form $L \rightarrow L + T$ and $L \rightarrow T + T$. However, from the results it cannot be excluded that anomalous phonon dispersion also exists in solid ^{4}He.

This work also presents a measurement of the attenuation of 1-GHz phonons in liquid ^{4}He at svp and at 23 bar. The results, which are in good agreement with existing work, show that anomalous phonon dispersion influences sound attenuation in ^{4}He at svp up to 0.8 K, while in ^{4}He at 23 bar the interaction of the sound wave with rotons is most important.

ACKNOWLEDGMENTS

We would like to express our gratitude to Prof. K. Dransfeld for his valuable support and advice. We also would like to thank H. Maris, J. Jäckle, and K. W. Kehr for helpful discussions during the course of this work.

One of us (P.B.) acknowledges financial support from Graduierten-Förderungsprogramm. This work was supported by Deutsche Forschungsgemeinschaft.

REFERENCES

1. M. Born and Th. von Karmann, *Phys. Z.* **13**, 297 (1912).
2. J. P. Franck and R. Wanner, *Phys. Rev. Lett.* **25**, 345 (1970).
3. R. H. Crepeau, O. Heybey, D. M. Lee, and S. A. Strauss, *Phys. Rev. A* **3**, 1162 (1971).
4. D. S. Greywall, *Phys. Rev. A* **3**, 2106 (1971).
5. V. J. Minkiewicz, T. A. Kitchens, F. P. Lipschultz, R. Nathans, and G. Shirane, *Phys. Rev.* **174**, 267 (1968).
6. R. A. Reese, S. K. Sinha, T. O. Brun, and C. R. Tilford, *Phys. Rev. A* **3**, 1688 (1971).
7. N. R. Werthamer, *Am. J. Phys.* **37**, 763 (1969).
8. N. S. Gillis, T. R. Koehler, and N. R. Werthamer, *Phys. Rev.* **175**, 1110 (1968).
9. N. R. Werthamer, *Phys. Rev. B* **1**, 572 (1970).
10. W. C. Kerr and A. Sjölander, *Phys. Rev. B* **1**, 2723 (1970).
11. H. Horner, *Z. Physik* **242**, 432 (1971).
12. J. Jäckle and K. W. Kehr, *Phys. Rev. Lett.* **24**, 1101 (1970).
13. L. Landau and G. Rumer, *Phys. Z. Sowjetunion* **11**, 18 (1937).
14. H. J. Maris, in *Physical Acoustics*, W. P. Mason and R. N. Thurston, eds. (Academic Press, New York, 1971), Vol. VIII, p. 279.
15. S. G. Eckstein, Y. Eckstein, J. B. Ketterson, and J. H. Vignos, in *Physical Acoustics*, W. P. Mason and R. N. Thurston, eds. (Academic Press, New York, 1970), Vol. VI, p. 259.
16. A. Akhieser, *J. Phys. (USSR)* **1**, 277 (1939).
17. H. H. Barrett, *Phys. Lett*, **21**, 623 (1966).
18. H. J. Maris, *Phys. Rev. A* **8**, 1980 (1973); **8**, 2629 (1973); **9**, 1412 (1974).
19. I. M. Khalatnikov and D. M. Chernikova, *Zh. Eksp. Teor. Fiz.* **41**, 1957 (1965) [*Sov. Phys.—JETP* **22**, 1336 (1966)].

20. I. M. Khalatnikov and D. M. Chernikova, *Zh. Eksp. Teor. Fiz.* **50**, 411 (1966) [*Sov. Phys.—JETP* **23**, 274 (1966)].
21. Yu. A. Matveyev, *Zh. Eksp. Teor. Fiz.* **65**, 1175 (1973) [*Sov. Phys.—JETP* **38**, 582 (1974)].
22. J. Wilks, *Liquid and Solid Helium* (Oxford University Press, Oxford, England 1967), Chapter 8.
23. J. Jäckle and K. W. Kehr, *Phys. Rev. Lett.* **27**, 654 (1971).
24. W. Kaiser and M. Maier, in *Laser Handbook*, F. T. Arecchi and E. O. Schulz-Dubois, eds. (North-Holland, Amsterdam, 1972), Vol. 2, p. 1077.
25. J. Pelous, C. Vedel, M. Bouissier, and L. Cecchi, *Phys. Lett.* **38A**, 73 (1972).
26. R. L. St. Peters, I. J. Greytak, and G. B. Benedek, *Opt. Commun.* **1**, 412 (1970).
27. G. Winterling and W. Heinicke, *Phys. Lett.* **27A**, 329 (1968).
28. P. Leiderer, P. Berberich, and S. Hunklinger, *Rev. Sci. Instrum.* **44**, 1610 (1973).
29. R. T. Beyer and S. V. Letcher, *Physical Ultrasonics* (Academic, New York, 1969).
30. M. A. Breazeale and J. Ford, *J. Appl. Phys.* **36**, 3486 (1965).
31. D. T. Blackstock, *J. Acoust. Soc. Am.* **39**, 1019 (1965).
32. E. M. Hogan, R. A. Guyer, and H. A. Fairbank, *Phys. Rev.* **185**, 356 (1969).
33. R. Berman, C. R. Day, D. P. Goulder, and J. E. Vos, *J. Phys. C* **6**, 2119 (1973).
34. B. M. Abraham, Y. Eckstein, J. B. Ketterson, and J. H. Vignos, *Cryogenics* **9**, 274 (1969).
35. B. M. Abraham, Y. Eckstein, J. B. Ketterson, M. Kuchnir, and P. R. Roach, *Phys. Rev. A* **1**, 250 (1970).
36. W. Heinicke, G. Winterling, and K. Dransfeld, *Phys. Rev. Lett.* **22**, 170 (1969).
37. B. M. Abraham, Y. Eckstein, J. B. Ketterson, M. Kuchnir, and J. Vignos, *Phys. Rev.* **181**, 347 (1969).
38. M. A. Woolf, P. M. Platzman, and M. G. Cohen, *Phys. Rev. Lett.* **17**, 294 (1966).
39. D. F. Brewer and D. O. Edwards, in *Proc. 8th Int. Conf. on Low Temp. Phys.*, R. O. Davies, ed. (Butterworths, London, 1963), p. 96.
40. H. J. Maris and W. E. Massey, *Phys. Rev. Lett.* **25**, 220 (1970).
41. R. K. Wehner, *Phys. Rev. A* **9**, 2625 (1974).
42. P. R. Roach, J. B. Ketterson, and M. Kuchnir, *Phys. Rev. Lett.* **25**, 1002 (1970); *Phys. Rev. A* **5**, 2205 (1972).
43. E. C. Svennson, A. D. B. Woods, and P. Martel, *Phys. Rev. Lett.* **29**, 1148 (1972).
44. O. W. Dietrich, E. H. Graf, C. H. Huang, and L. Passell, *Phys. Rev. A* **5**, 1377 (1972).
45. L. P. Pitaevskii, *Zh. Eksp. Teor. Fiz.* **36**, 1168 (1959); [*Sov. Phys.—JETP* **9**, 830 (1959)].
46. J. Jäckle and K. W. Kehr, *Phys. Kond. Materie* **16**, 265 (1970).
47. S. Hunklinger, P. Leiderer, and P. Berberich, in *Light Scattering in Solids*, M. Balkanski, ed. (Flammarion Sciences, Paris 1971), p. 453; P. Leiderer, P. Berberich, S. Hunklinger, and K. Dransfeld, in *Low Temperature Physics—LT13*, K. D. Timmerhaus, W. J. O'Sullivan, and E. F. Hammel, eds. (Plenum, New York, 1974), Vol. 2, p. 53.
48. G. Ahlers, *Phys. Rev. A* **2**, 1505 (1970), and references quoted therein.
49. K. Brugger, *J. Appl. Phys.* **36**, 768 (1965).
50. Y. Hiki and A. V. Granato, *Phys. Rev.* **144**, 411 (1966).
51. R. R. Rao and R. Srinivasan, *Phys. Stat. Sol.* **29**, 865 (1968).
52. C. C. Ackerman and R. A. Guyer, *Ann. Phys. (N.Y.)* **50**, 128 (1968).
53. P. G. Klemens, *J. Appl. Phys.* **38**, 4573 (1967).
54. P. G. Klemens and F. P. Lipschultz, *Phys. Lett.* **30A**, 127 (1969).
55. J. F. Jarvis, D. Ramm, and H. Meyer, *Phys. Rev.* **170**, 320 (1968).
56. N. G. Mills, R. A. Sherlock, and A. F. G. Wyatt, *Phys. Rev. Lett.* **32**, 978 (1974).
57. R. C. Dynes and V. Narayanamurti, *Phys. Rev. Lett.* **33**, 1195 (1974).